Available online at www.sciencedirect.com

ScienceDirect

Biosurface and Biotribology 2 (2016) 102–113

www.elsevier.com/locate/bsbt

An *in vitro* study of the wear behaviour of dental composites

J.A. Arsecularatne, N.R. Chung, M. Hoffman*

School of Materials Science and Engineering, UNSW Australia, Sydney 2052, Australia

Received 15 June 2016; received in revised form 1 September 2016; accepted 5 September 2016

Abstract

Use of dental resin composites in restorative dentistry has increased significantly in recent years. While wear may be of minimal importance for small to medium size composite restorations, failure rates are higher for large restorations. Moreover, wear is a significant mode of posterior restoration failure for patients with bruxing and clinching habits. However, in spite of previous *in vitro* studies, the mechanisms associated with the wear of these composites are not yet clearly identified. Accordingly, the wear behaviours of three different glass-polymer dental composite materials were studied *in vitro* and the associated mechanism(s) were investigated in-depth.

Reciprocating sliding wear tests were carried out using these composites where a self-mating composite cusp was sliding on a flat-surface sample. The wear loss was quantified using profilometry and the wear scar surface and subsurface were analysed using electron microscopy techniques to reveal the underlying wear mechanisms. The composites' mechanical properties were assessed using nanoindentation.

The results revealed that two different wear mechanisms were dominant for the composites tested: fatigue wear for the anterior/posterior composites and, abrasion due to lateral crack formation and filler particle pull out for the anterior composite.

Keywords: Wear mechanism; Electron microscopy; Dental composite

1. Introduction

Dental resin composites containing filler particles (e.g., borosilicate glass, colloidal silica, etc.) in a polymer matrix (e.g., bisphenol A glycidyl methacrylate (BisGMA), triethylene glycol dimethacrylate (TEGDMA), etc.) are commonly used to restore cavities and non-carious cervical lesions (NCCLs) and to replace the missing tooth tissue that has been worn away by grinding [1–3]. The functions of filler particles are to reduce the polymerisation shrinkage on setting and to improve the composite's wear resistance. Use of these composites in restorative dentistry has increased significantly in recent years due to their good aesthetics, the ability to bond to tooth structures and the need for an amalgam alternative.

Early dental resin composites in the 1970s which contained large filler particles (above 10 μm diameter) showed rapid wear when used on the biting surfaces of posterior teeth [2]. Significant improvements have been made with the introduction of composites with medium size filler particles (e.g., 2.5 μm) in the mid-1980s and more recent micro/nano-hybrid composites, and wear of dental composites has been substantially reduced. While wear may be of minimal importance for small to medium size restorations, failure rates are higher for large restorations, particularly, those involving the replacement of functional cusps, which are routinely performed [4]. Moreover, wear is a significant mode of posterior restoration failure for patients with bruxing and clinching habits [5,6].

Since bruxism and erosion are often associated with severe tooth wear, restorations placed on worn teeth are also considered to subject to same wear processes [7]. However, the available evidence on the longevity of restorations originates from studies in which severe tooth wear was usually an exclusion criterion and hence the results of these studies do not reveal the restoration longevity of severe wear cases. In addition, the available literature on restorative treatment of patients with severe tooth wear is also very limited [7]. One recent study has revealed that, despite considerable restorative wear observed, improved retention of

*Corresponding author. Fax: +61 2 9385 6545.
Peer review under responsibility of Southwest Jiaotong University.

http://dx.doi.org/10.1016/j.bsbt.2016.09.002

Table 1
Details of the three dental composites and the average specimen surface roughness values.

Composite	Intended application	Filler particles, %	Particle size (nm)	Specimen surface roughness (R_a, μm)	
				Ground	Polished
DC-1	Anterior/Posterior	Alumino silicate glass, 61 %vol	50–1000	0.043 ± 0.009	0.022 ± 0.004
DC-2	Anterior/Posterior	Strontium glass, 61 %vol	50–2000	0.055 ± 0.008	0.015 ± 0.001
DC-3	Anterior	Silica, 51 %wt	20–100	0.034 ± 0.006	0.049 ± 0.01

hybrid composite restorations compared to micro-filled composite ones [8].

From the above discussion, it is clear that there is a requirement for further improvement of wear behaviour of dental composites through qualitative/quantitative assessment and identification of the associated wear mechanisms. Investigators in previous studies have stated that the dominant wear mechanism(s) of these composites are abrasion and fatigue [9] or fatigue [10,11] or abrasion due to microcutting or microcracking [12] or delamination [13]. Another study has concluded that delamination is dominant for more brittle composites under higher loads [14]. These indicate that the mechanisms associated with the wear of dental composites are not yet clearly understood. The reasons for this can be summarised as follows: while some researchers have assumed the dominant wear mechanism [9–12], others [13,14] have restricted their study to the analysis of wear surface topography by scanning electron microscopy (SEM). It appears that only one study carried out in early 1980 [11] analysed the wear scar subsurface damage of dental composites using silver staining process and optical microscopy.

The present study attempts to overcome the aforementioned disadvantages by carrying out an in-depth analysis of composites' wear surface and subsurface by SEM and transmission electron microscopy (TEM) to reveal the underlying wear mechanism. Additionally, the observed tribological behaviour of these composites will also be related to their fracture behaviour. The findings of this research should in turn facilitate the development of novel composite materials with improved wear properties.

Previous *in vitro* dental composite wear studies have used various tooth wear simulators (e.g., Oregon Health Sciences University wear simulator [15]) and standard tribometers (e.g., pin-on-disc, reciprocating). However, simple pin-on-disc tests are not considered to be representative of the wear processes that occur in the oral environment [16]. Although wear simulators seem more representative of the processes *in vivo*, they are not widely available, possibly due to the high initial cost [14]. Moreover, a carefully controlled round-robin test [17] that used five different wear simulators revealed 'tremendous' variations in the wear ranks of tested materials among different simulators although publications relating to three of these simulators attempted to establish clinical correlations. Thus no universally accepted in vitro method is currently available for evaluating the wear of dental materials which totally simulated the clinical behaviour [18]. Conversely, even though a reciprocating tribometer does not provide a replica of *in vivo* loading, it facilitates similarities in the wear process, isolates a more relevant range of factors and provides excellent repeatability. It was hence chosen for the present experiments.

Use of various antagonist materials for *in vitro* wear testing of composite dental materials has also been reported in literature. These materials include stainless steel, chromium steel, human enamel, dental ceramic, common ceramic, e.g., alumina [11–14]. All these materials are known to have disadvantages [13]: steels and ceramics having properties considerably different to those of human enamel; human enamel with size limitations, irregular shape, variable structure and properties. Accordingly, in the present work, self-mating dental composite specimens (i.e., both sliding partners made of same composite material) will be used. It can be argued that such self-mating dental composite specimens in sliding contact have clinical relevance since a composite cusp sliding on a composite fossa can occur in the oral environment.

2. Materials & methods

The dental composite specimens required for the tests DC-1, DC-2 and DC-3 (Table 1) were prepared in teflon moulds and were cured using blue light: 20 s per 2 mm thickness (Radii plus, SDI Limited, Bayswater VIC, Australia). Prior to the *in vitro* wear tests, nanoindentation tests were carried out to obtain the mechanical properties, in particular, hardness and elastic modulus.

2.1. Dental composite specimen preparation

2.1.1. Nanoindentation

For these tests, short cylindrical composite specimens (4 mm height and 4 mm diameter) were used. In order to obtain the final geometry, a flat surface of an original specimen was first ground using 2500 grade SiC paper to improve its flatness. It was then used to glue the specimen on to a perspex pin using commercial superglue with 20-24 hours allowed for adequate curing of superglue and to obtain a stronger bond.

The free/exposed flat surface of each cylindrical specimen was then prepared for nanoindentation testing. It was initially ground using 1200, 2500, 4000 grades SiC paper followed by polishing with 1 μm diamond suspension. For these tests, six specimens in total (2 specimens per composite) were prepared.

2.1.2. Wear tests

For these tests two sample geometries suitable for *in vitro* reciprocating wear testing were prepared: short cylindrical samples (4 mm height and 4 mm diameter) as flat surface

specimens; conical samples (4 mm diameter base and 4 mm height) as cusp specimens. During a wear test, a cusp tip slid on a flat surface specimen.

In order to obtain the final sample geometries, a flat surface of each original cylindrical specimen and the circular base of each conical specimen were first ground using 2500 grade SiC paper to improve their flatness. These ground surfaces were then used to glue the specimens on to perspex pins (one sample per pin) using superglue as described earlier.

The free/exposed flat surface of each cylindrical specimen was then prepared for wear tests by grinding with 1200, 2500, 4000 grades SiC paper sequentially. One half of these specimens were further polished with 1 μm diamond suspension. Thus specimens with two final surface finishes were tested for each composite: ground with 4000 grade SiC paper or polished with 1 μm diamond suspension. In total, 24 flat surface specimens were prepared for the wear tests.

In order to prepare the cusp specimens for wear testing, the tip of each conical specimen was carefully ground (with 2500 and 4000 grades SiC paper) to obtain a contact area of approximately 0.5 mm diameter with rounded edge. The contacting areas of one half of these specimens were further polished with 1 μm diamond suspension. All grinding and polishing processes were carried out under well hydrated conditions. In total, 24 cusp specimens were prepared for the wear tests.

2.2. Testing

2.2.1. Surface roughness

The surface roughness R_a of the ground/polished flat surface specimens was measured using a profilometer (Surftest SV-600, Mitutoyo Corporation, Tokyo, Japan) with a diamond stylus (tip radius of 5 μm) operating at a velocity of 0.1 mm/s.

2.2.2. Nanoindentation

These experiments were performed using an instrumented indentation system (Ultra Micro Indentation System, UMIS-2000, CSIRO, Australia) with a Berkovich diamond tip. Before the experiments, the indenter area function was established by making over 150 indents on a fused silica sample under loads from the range 1–250 mN.

A perspex pin with a composite sample was mounted on a magnetic stainless steel holder. This holder was then securely mounted on the UMIS test table which contained a magnetic stage. The area selected for the indentations was at least 300 μm away from the edge of specimen surface. That way, it was expected to indent the sound composite material avoiding any (outer) surface abnormalities.

The maximum indentation load selected was 200 mN (a higher load range was selected because of the nonhomogeneous nature of these materials and to obtain more representative mechanical properties) with the spacing between indentations 100 μm. On each flat surface specimen, one or two locations were chosen for indentation. At each location, 12 indentations were performed for assessing the variability of the measured mechanical properties and to determine the average values. For each indentation test, 20 loading/unloading steps were used. Additionally, a hold time of 0.1 s was specified between each loading step. The indentation loading rate was ~150 nm/s which was the maximum for the instrument. Since bulging of the load-displacement curve was observed on unloading during preliminary tests, a 10 s hold at maximum load was introduced to overcome this problem.

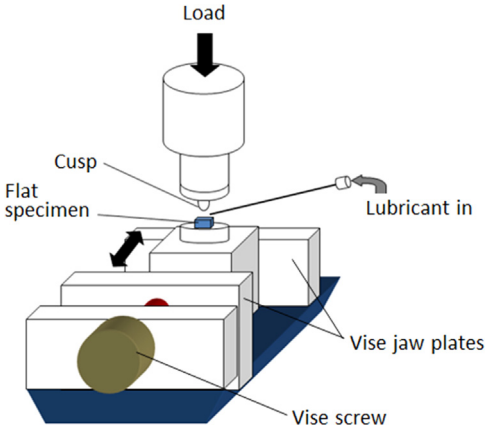

Fig. 1. Set-up for wear testing.

Following an indentation test, the hardness (H) and the reduced elastic modulus (E^*) were calculated as proposed by Oliver and Pharr [19].

2.2.3. Wear testing

Reciprocating wear tests were carried out on a tribometer with a reciprocating module (CSEM, Peseux, Switzerland) for 2250 cycles (approximately 33 min) with self-mating composite specimens (e.g., DC-1 cusp sliding against a DC-1 flat-surface sample) with a stroke of 2 mm. In the test setup, a perspex pin with cusp attached was mounted on a cylindrical stainless steel holder which was held on the tribometer arm. The perspex pin with flat specimen attached was mounted on a cubic stainless steel holder which was held in a vice on the reciprocating module. Thus the cusp and the flat composite specimen reciprocated against each other during a test (Fig. 1). Mating cusp and flat surface pairs had same surface preparation (i.e., either both of them were ground or both of them were polished).

During testing, a normal load[1] of 2, 5 or 10 N was applied. The linear speed varied sinusoidally during the stroke and the overall frequency was 66 cycle/min. Artificial saliva (Table 2) at pH 7 (adjusted using sodium hydroxide solution) and at 37 °C was used as the lubricant which was guided to the wear area by a hypodermic needle. A flow rate of 90 ml/h was set using an infusion pump (Imed Gemini PC-1, Alaris, San Diego, USA) and the lubricant was not recycled. The coefficient of friction was continuously recorded during testing.

The contact area of a cusp before and after a wear test was measured from images obtained using an optical microscope (Nikon Eclipse ME600L, Japan). The substance loss due to wear on each flat-surface sample was determined using the wear scar dimensions which were measured by a profilometer (Surftest SV-600, Mitutoyo Corporation, Tokyo, Japan) with a

[1]The corresponding contact pressures under these loads are in the range 8–55 MPa which are comparable to those reported for natural dentition (5–20 MPa) [20].

Table 2
Composition of artificial saliva [21].

Compound	NaCl	KCl	$CaCl_2.2H_2O$	$NaH_2PO_4.2H_2O$	$Na_2S.9H_2O$	Urea	Distilled water
Quantity	0.4 g	0.4 g	0.795 g	0.78 g	0.005 g	1 g	~998 ml

diamond stylus (tip radius of 5 μm) operating at a velocity of 0.1 mm/s. The wear scar profiles were obtained perpendicular to the sliding direction. A minimum of four profiles were obtained for each wear scar to determine its average depth.

In order to assess the variability of the measured parameters, repeated tests were made under selected conditions. The composite samples following wear testing were dried overnight at 35 °C for FIB/SEM and TEM analyses.

2.3. Analyses

The wear scar on selected flat surface composite specimens was analysed using electron microscopy techniques: scanning and transmission electron microscopy (SEM and TEM), focussed ion beam (FIB) milling and energy dispersive X-ray (EDX). Firstly, a thin gold coating (~50 nm thickness) was applied on the composite wear surface approximately 15 min before the start of the FIB/SEM analysis and TEM foil preparation to protect the surface from gallium ion beam damage and to minimise charge build-up.

2.3.1. FIB/SEM

Subsurface sectioning and imaging of the sample surface was performed using a dual electron beam and FIB system (Nova Nanolab 200, FEI Company, Hillsboro OR, USA). Sections for SEM imaging were prepared perpendicular to the sliding direction and wear surface. At the start, a layer of platinum ~1 μm thick was deposited on to the area of interest to further protect the composite surface from ion-beam damage during the milling process. During FIB sectioning, a high current 5000–7000 pA gallium ion beam was first used to mill the specimen surface and create a wedge-like trench of 5 μm long and 15 μm wide, with maximum depth of 5 μm. The resultant 'rough' subsurface profile was then cleaned and polished at reduced currents, 1000 pA and 300 pA respectively, to remove any deposited particles and to obtain a smooth surface for observation and imaging using SEM.

FIB/SEM imaging was also carried out on radial subsurface sections made on ground or polished specimen surfaces away from wear scar for comparison.

2.3.2. TEM

TEM foils were also prepared using the above dual electron/FIB system. Foils were prepared from the wear surface of selected composite specimen perpendicular to the sliding direction. Additionally, foils were also made on the specimen surfaces away from the wear scar for comparison.

The TEM foil preparation procedure again started with the deposition of a ~1 μm thick platinum layer on the area of interest. A 'rough' mill was then performed with a high current (7000 pA) during which parallel trenches were cut to obtain a section ~3 μm thick. A number of 'fine' mills were then performed at a reduced current (~1000 pA) and the section thinned down to ~1 μm thickness. In order to isolate the specimen, its bottom and parts of left and right edges were cut free at a 7° tilt. Final mills were carried out at further reduced currents (100–300 pA), reducing the thickness of the section down to ~100 nm. Then one side of the electron transparent foil was cut free. A micro-manipulation lift-out procedure was then used to transport the foil to a carbon coated copper grid for subsequent TEM observations which were made using a field emission transmission electron microscope (FEI Philips CM200). This equipment also had an EDX spectroscopy system interfaced to it which allowed chemical analysis of a selected area of the foil.

3. Results

3.1. Surface roughness

The measured surface roughness Ra values reveal smoother surfaces for anterior/posterior composites DC-1 and DC-2 following polishing (Table 1). However, for the anterior composite DC-3, polishing did not improve its surface roughness.

3.2. Nanoindentation

The obtained nanoindentation hardness (H) and modulus (E^*) results did not show a significant variability from location to location across a specimen of a particular composite. However, they showed considerable variations between different composite materials (Fig. 2). As expected, measured H (Fig. 2(a)) and E^* Fig. 2(b) values for the anterior/posterior composites DC-1 and DC-2 are much higher than those for anterior composite DC-3.

Under 200 mN load, measured H and E^* for the present anterior/posterior composites (DC-1 and DC-2) were in the range 0.8–0.9 GPa and 18–21 GPa, respectively, while these values for the anterior composite DC-3 were in the range 0.30–0.35 GPa and 7–8 GPa, respectively. For human dental enamel, reported H and E^* were 4.3 ± 0.5 GPa and 117 ± 21 GPa, respectively [22]. These nanoindentation results show that the tested dental composite materials are considerably softer and less stiff than human dental enamel.

3.3. Wear loss and coefficient of friction

The measured wear volumes following 2250 reciprocating cycles for the three dental composite specimens with varying surface preparations (ground/polished) are shown in Fig. 3. It was noted that the measured contact area of some the cusps

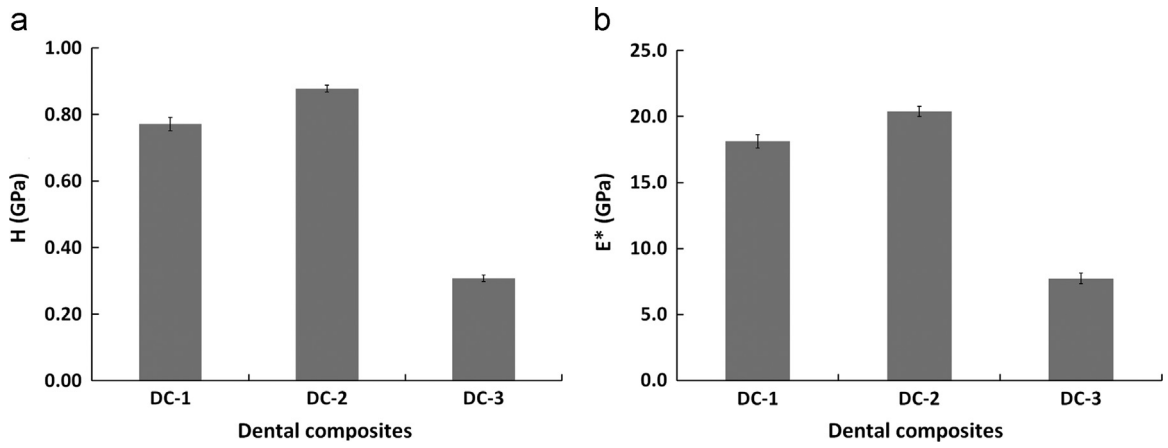

Fig. 2. Measured nanoindentation mechanical properties for the three composites: (a) hardness; (b) reduced elastic modulus. The error bars represent standard deviations.

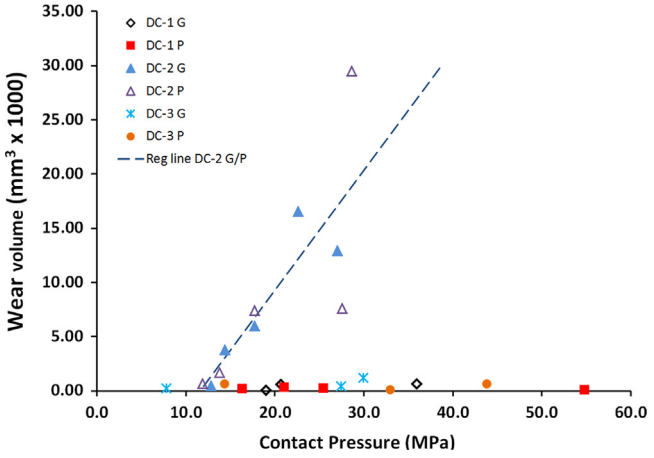

Fig. 3. Variations of measured wear volume versus contact load for dental composites (G – ground specimens; P – polished specimens).

before and after a wear test were considerably different in that the latter had increased due to wear. To account for this variation, average contact pressure (calculated using contact load and measured contact area) was used for the horizontal axis in Fig. 3.

In Fig. 3, the symbols represent the experimental results. It can be seen that the measured wear volumes for the DC-2 composite (for both ground and polished surfaces) are much higher than those for DC-1 and DC-3. Moreover, the wear volume for DC-2 depends on the contact load in that an increase in load increases the wear loss. However, wear volumes for composites DC-1 and DC-3 show little or no dependency on contact load.

In spite of the scatter which is often associated with experimental wear measurements [23], the measured wear volume for all DC-2 specimens (ground or polished) generally follow a single curve which can be represented by a linear relation (the regression line in Fig. 3 has a correlation coefficient greater than 0.65). It indicates a negligible influence of polished/ground flat surface specimen preparation on measured steady state wear rate. It also indicates that polishing of an initially ground DC-2 surface does not influence the composite's wear behaviour.

For the three dental composites, the average coefficient of friction values measured were in the range 0.03–0.09 (these are steady state values excluding the initial 'run-in' stage where friction increased rapidly). These values did not show a significant variation depending on the composite and/or contact load.

3.4. Wear surface topography (SEM)

Fig. 4 shows representative SEM images of wear surfaces obtained for the three composites under 10 N load for specimen with 'ground' surface finish (Table 1). For DC-1 (Fig. 4(a)) and DC-2 (Fig. 4(b)) composites, the formation of flake shaped wear particles (arrowed) can be seen. A significantly higher number of partially detached wear particles was observed on the wear surface of DC-1 than that of DC-2. The wear surface is rough at locations where these wear particles were removed (arrow heads). Such topography seems to indicate a dominant fatigue wear mechanism. For DC-3, only some oriented grooves parallel to the sliding direction were observed (Fig. 4(c)). These oriented grooves indicate an abrasive wear mechanism.

Under lower contact loads (2 and 5 N), the wear surface topography also indicated a dominant fatigue wear mechanism for composites DC-1 and DC-2 though some abrasion was also noted under 2 N load. For the DC-3 composite, the wear surface topography indicated a dominant abrasion mechanism under 2 and 5 N loads.

3.5. FIB/SEM

Fig. 5 depicts an SEM image of a dental composite (DC-1) wear surface which was used for FIB/SEM analysis and TEM foil preparation. It shows an FIB section (top-right inset) and a TEM foil (bottom-left inset) prepared for subsurface observations perpendicular to the sliding direction and top flat surface.

Subsurface images of the wear scar on flat surface DC-1 and DC-2 specimens from the region where surface cracks (possible fatigue wear (Fig. 4(a) and (b))) observed are shown in Fig. 6(a) and (b). In both cases, relatively larger subsurface cracks can be seen (arrowed). They have opened up possibly due to the repeated sliding of the cusp and relatively higher

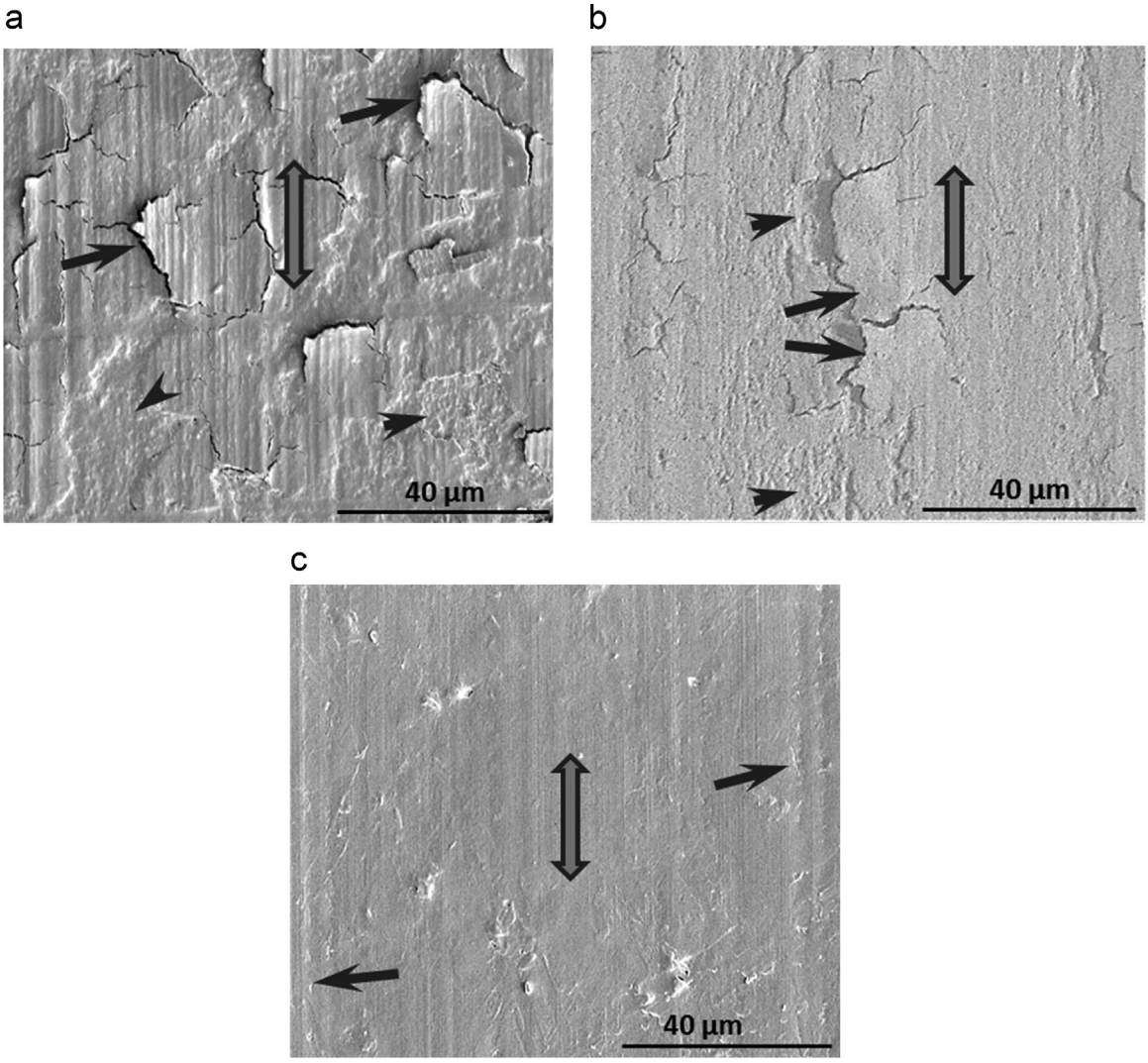

Fig. 4. Wear surface topography under 10 N load for the three composites: (a) DC-1; (b) DC-2; (c) DC-3. Double ended arrow indicates the sliding direction; arrows indicate formation of flake shape wear debris; arrow heads indicate rough surface following wear particle removal.

tensile stress closer to the surface. These relatively large subsurface cracks are likely to generate large flake shape wear particles: a characteristic of fatigue wear. Subsurface profiles of the wear scar of DC-3 specimens show an uneven wear surface without any subsurface cracks. A typical profile is depicted in Fig. 6(c).

Subsurface profiles made on the flat surface dental composite specimens outside the wear scar and imaged using SEM indicated a relatively smooth surface without any subsurface cracks.

3.6. TEM

The bright field TEM image in Fig. 7(a) was obtained from a foil made on the wear scar of a DC-1 composite specimen in a region that indicated recent removal of a wear particle due to delamination/fatigue e.g., Fig. 4(a) (arrow). The filler particles in these images (Fig. 7) were confirmed by an analysis of their compositions using EDX. Protruded filler particle surfaces indicate crack propagation through the matrix, not through the particles (Fig. 7(a)). Interface debonding is not observed in this image. The images in Fig. 7(b) were obtained from a foil made radially on the wear scar of a DC-1 specimen in a region that indicated surface cracking (Fig. 4(a)). A subsurface crack has propagated mainly through the resin matrix closer to the surface and the filler particles in the crack path are intact. This indicates that the crack did not propagate through the filler particles but around them. The crack tip (arrow head) is clearly within the resin matrix and a filler particle well ahead of the crack tip shows some debonding (arrow). The crack propagation and/or particle interface debonding seem to occur closer to the surface, i.e., only up to a depth of 500 nm below the surface.

The bright field TEM image in Fig. 7(c) was obtained from a foil made radially on the wear scar of a DC-2 specimen. Unlike DC-1 discussed above, greater particle debonding can be noted. Moreover, for DC-2, subsurface cracks seem to initiate at the filler particle–resin matrix interface (Fig. 7(d)). It can also be seen that the crack initiation or particle debonding can occur at a depth approximately 1 μm below the surface (which is much deeper than that seen for DC-1). This will cause generation of thicker wear particles for DC-2, compared to DC-1.

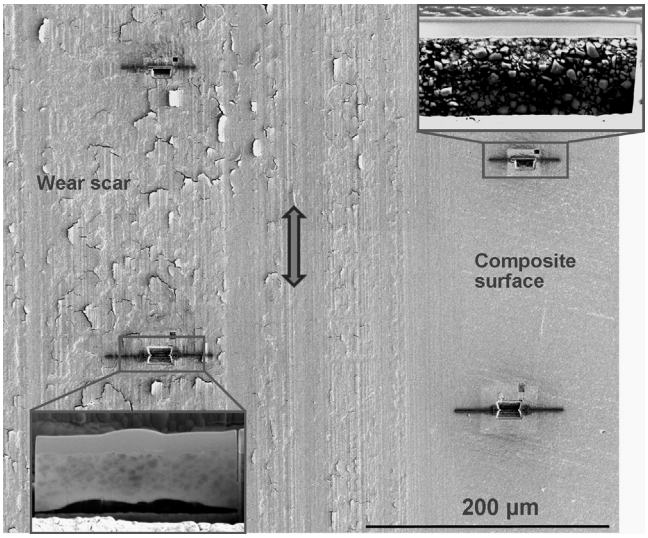

Fig. 5. DC-1 composite surface following wear testing with FIB sites for subsurface observations (top-right inset) and TEM foil preparation (bottom-left inset).

For DC-1, the TEM images from foils prepared outside the wear scar revealed a relatively flat top surface and no filler particle debonding closer to the surface. However, for DC-2, some of the filler particles at the surface have started to debond and the (ground) surface was not as smooth as that of DC-1 possibly due to pull out of some of the filler particles during grinding. This may have caused the relatively large difference between the surface roughness values of ground and polished surfaces of the DC-2 composite (Table 1).

The bright field TEM image in Fig. 7(e) was obtained from a foil made radially on the wear scar of a DC-3 specimen. At 'A', a relatively large wear particle has been removed possibly due to lateral cracking and/or particle pull out. The concave surface depressions (arrowed) indicate sub-micrometre scale wear particle formation due to lateral crack extension (a wear particle formed but not yet removed by the sliding cusp can be seen at 'B'). Pull out of relatively small filler particles in DC-3 composite is the likely cause of observed increase in surface roughness following polishing (Table 1).

Additionally, TEM images of the ground/polished DC-3 specimen surface from locations well away from the wear scar also revealed concave surface depressions similar to those observed on the wear surface (Fig. 7(e)) discussed above. These TEM results indicate that the dominant wear mechanisms for the DC-3 composite during sliding contact (in a wear test) and in grinding/polishing (during specimen preparation) are similar. Such surface depressions have also been observed on the wear surface of a glass ceramic dental material when abrasion was the dominant wear mechanism [24]. These results indicate that abrasion is the dominant wear mechanism for the DC-3 composite.

Considering that little or no particle debonding was observed in DC-1, filler particles in this composite seem strongly bonded to the resin matrix. However, in DC-2, the particles seem weakly bonded to the matrix. Considering that some particle debonding was observed in DC-3 (but less particle debonding than in DC-2), its interface bonding strength seems to be between those of DC-1 and DC-2.

4. Discussion

4.1. Comparison of wear loss of dental composites and enamel

In this section, an attempt will be made to compare the quantitative wear loss for the tested dental composites with that of human dental enamel under similar conditions.

In Fig. 8, in addition to the three dental composites (with artificial saliva (AS) lubricant) considered in the present work, wear volume measurements obtained for human dental enamel with lubricants of saline, citric acid (CA) and acetic acid (AA) are also included. Note that the artificial saliva and saline lubricants were at pH 7 while citric acid and acetic acid were at pH 5.5. The enamel wear results for citric acid and acetic acid lubricants were taken from Wu et al. [25] who used the same equipment, testing configuration and similar test parameters as used in the present study. The results for the saline lubricant were taken from Eisenburger and Addy [26]. Their testing configuration/parameters have some similarities to those of present study, e.g., number of reciprocating cycles was 2280 (compared to 2250 in present study) and a cusp was sliding on a flat surface specimen. The results from [26] were included in Fig. 8 since, for enamel cusp on enamel flat surface test configuration, no wear data are available for artificial saliva lubricant.

It can be seen that the measured wear rates for the dental composites DC-1 and DC-3 with artificial saliva lubricant in the present study are similar to those reported for human enamel with citric acid (at pH 5.5) and acetic acid (at pH 5.5) lubricants. The measured wear rates for the dental composite DC-2 with artificial saliva lubricant in the present study are much higher than those reported for human enamel with the above acidic lubricants but lower than those for human enamel with saline lubricant.

4.2. Wear behaviour of composites and associated mechanisms

Human dental enamel is considered to be highly wear resistant despite complex and changing oral conditions [1]. Accordingly, an ideal restorative material is expected to possess similar tribological behaviour to enamel which will then minimise the potential for increased wear to alter the vertical dimension of occlusion and, reduced strength of teeth/restorations and increased plaque accumulation [27]. Of the three dental composites tested in the present study, DC-1 and DC-2 are intended for anterior/posterior restorations while DC-3 for anterior restorations. The wear behaviour of posterior composites under high contact loads is of great interest due to the demands of bruxist individuals [4,7].

Although teeth suffer both two-body (attrition) and three-body (abrasion) wear in the oral environment [1], attrition resulting from bruxism is considered to play a major role in patients with severe wear [7]. Thus the present study considered only the two-body

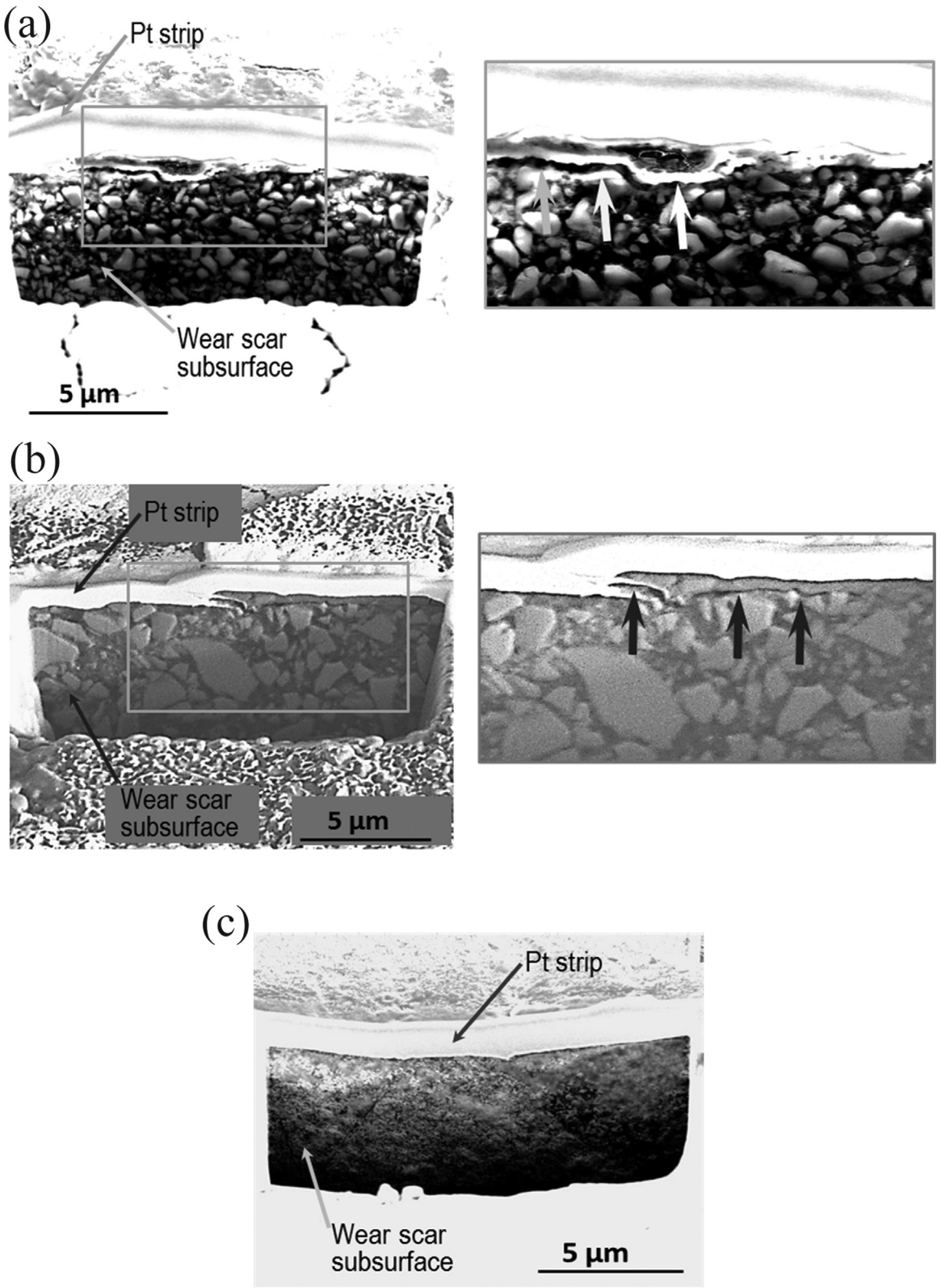

Fig. 6. Wear scar subsurface sections under 10 N load for the three composites (arrows indicate a subsurface crack): (a) DC-1; (b) DC-2; (c) DC-3.

condition following previous investigators [12,28]. This enabled the present authors to investigate the wear behaviours in-depth and to identify the associated wear mechanisms. Moreover, in the present wear tests, sliding occurred under constant load since it allowed an investigation of the influence of load on the wear behaviour.

The FIB/SEM/TEM analyses of present study confirmed that the filler particle size of composites DC-1 and DC-2 are similar (in the range 0.05–2.0 µm) while that of DC-3 is much smaller (20–100 nm). Yet the wear rates of composites DC-1 and DC-3 are similar while that of DC-2 is much higher. These

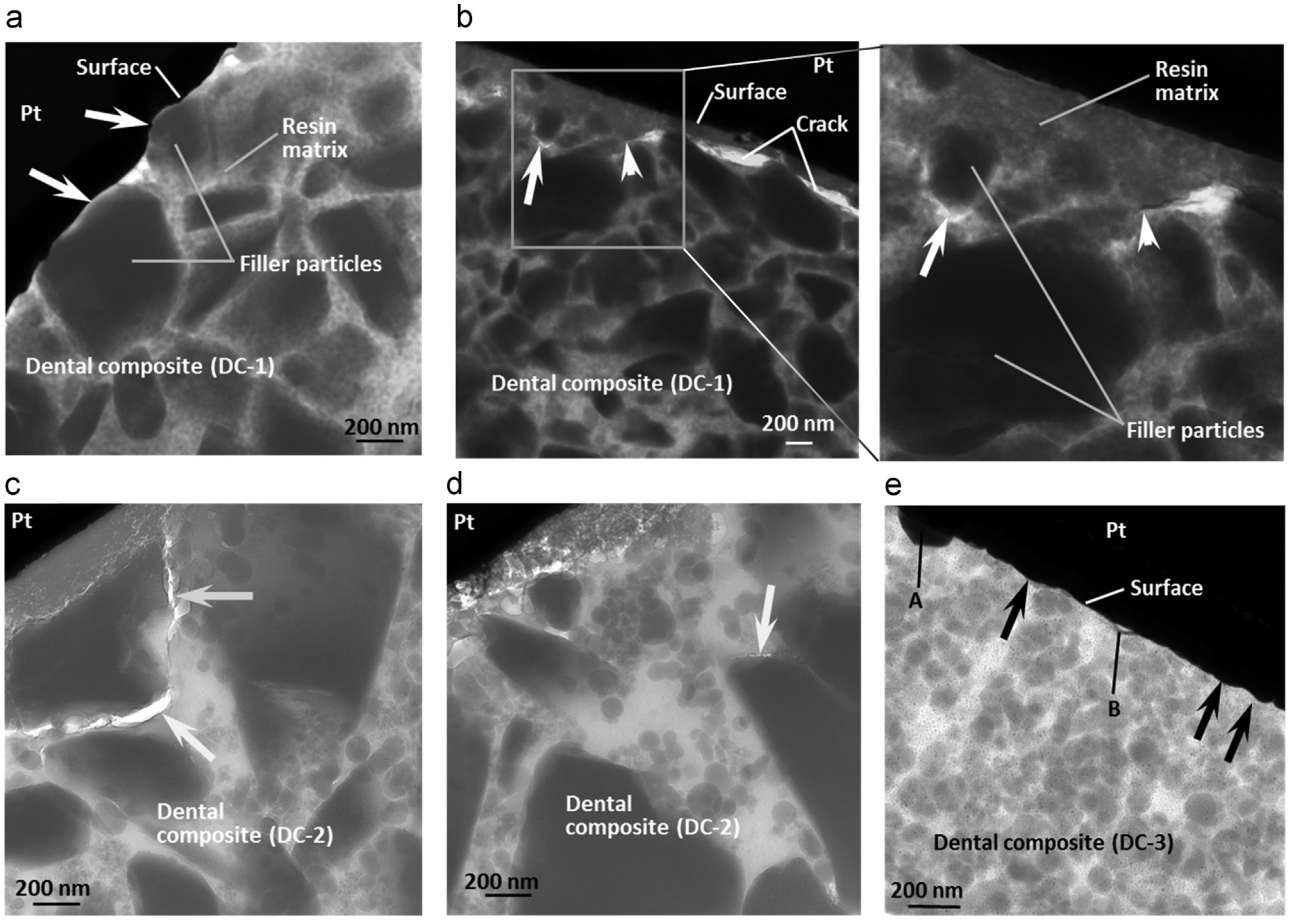

Fig. 7. TEM analysis: (a) Wear surface and subsurface of DC-1 composite (arrows indicate protruded filler particles at the surface); (b) Subsurface crack propagation in DC-1 during wear, a partially debonded filler particle (arrow) and crack tip (arrow head); (c) Wear surface and subsurface of DC-2 composite (arrows indicate crack propagation along particle-matrix interface); (d) Possible crack initiation (arrowed) in the subsurface of DC-2 composite; (e) Wear surface and subsurface of DC-3 composite (arrows indicate concave surface depressions).

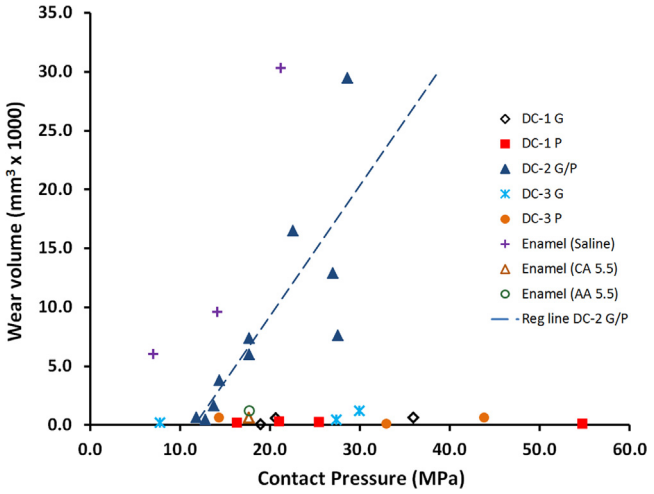

Fig. 8. Comparison of measured wear volume for dental composites and for human dental enamel with different lubricants (AA – acetic acid; AS – artificial saliva; CA – citric acid; DW – distilled water).

results do not necessarily support the view that larger particle sizes have an unfavourable effect on the wear resistance of dental composites [13].

Compared to enamel wear surfaces observed in previous studies [25,29], in the present study, a large number of partially detached flake shaped wear particles were seen on the wear surfaces of the DC-1 composite (Figs. 4(a) and 5). However the measured wear rate for this composite was low and no/little increase in the wear rate with increasing load was observed (Fig.3). Considering the clear subsurface crack formation observed on the wear scar (FIB/SEM and TEM analyses in Sections 3.5 and 3.6, respectively), wear of DC-1 seems to occur by a fatigue mechanism. This is supported by the results of Truong et al. [10] who investigated fatigue crack propagation in notched dental composite specimens under cyclic loading. Based on the assumption that microcrack growth in the subsurface damage layer was the precursor of wear, dynamic fatigue resistance combined with fracture toughness were used to explain the clinically observed wear of these composites, e.g., composites with higher fracture resistance/toughness were also found to possess a higher wear resistance. It appears that high fracture toughness and/or fatigue resistance retarded the formation of large wear particles which in turn reduced the material loss from the composite's sliding surface. The large number of partially detached wear particles observed on the wear surface and the measured low

wear rate for DC-1 composite compared to enamel wear surfaces support the above argument.

It thus appears that composite DC-1 possesses a high fracture toughness and/or fatigue resistance. It is also likely that the chemistry of its matrix and the degree of salinization are the major factors contributing to this enhancement of fatigue resistance [10]. One of the high fracture resistant composites tested by Truong et al. [10] had 50% higher fracture toughness (and corresponding high wear resistance) than one with lower fracture resistance. It appears that, due to the presence of contiguous particle networks in a composite (e.g., present composite DC-1), the stress field at the crack tip becomes less localised and energy dissipation can occur through a crack pinning mechanism in a larger volume resulting in a higher fracture resistance [10,30]. Additionally, for composite DC-1, the present TEM analysis also revealed filler particle debonding well ahead of the crack tip (Fig. 7(b)). Such debonding of filler particles gives rise to crack tip blunting, a mechanism considered to further increase the composite's fracture toughness [31].

Compared to composite DC-1, the wear surface of DC-2 showed less partially detached large wear particles (Fig. 4). In the present FIB/SEM and TEM analyses (Sections 3.3 and 3.4), clear subsurface crack formation and interface debonding was observed in DC-2. Although the measured wear rate for DC-2 increased at high load, the observed increase is lower than that for human enamel in a saline environment (Fig. 3) with associated delamination wear mechanism [32]. Additionally, the measured coefficient of friction for the dental composites was lower (in the range 0.03–0.09) compared to human enamel during delamination wear (0.1–0.4). These indicate that the wear mechanism associated with composite DC-2 was also fatigue. However, it possessed lower fracture toughness and a lower fatigue resistance compared to composite DC-1. Although interface debonding was observed in DC-2, it appears to display the behaviour of a more brittle composite material. For toughening of a composite by crack pining, a minimum adhesion between filler particles and resin matrix is required [31], and the filler particle–matrix adhesion in DC-2 seems to be inadequate. It is also possible that the residual tensile stresses at the particle–matrix interface due to polymerisation shrinkage amplify the stress intensity thereby reducing the overall toughness of DC-2 [33]. The present work reveals that even when the same wear mechanism (fatigue) dominating, two composites can show considerably different wear rates which is mainly influenced by filler-matrix interface debonding.

For the anterior composite DC-3, nanoindentation results revealed a much lower elastic modulus for DC-3 than for DC-1 or DC-2 (Fig. 2). Since the magnitude of Hertzian stresses depend on the elastic modulus, a lower elastic modulus decreases the onset of fatigue/delamination wear in DC-3 [24]. The present FIB/SEM and TEM results revealed that the dominant mechanism of DC-3 was abrasion due to lateral crack formation/extension and particle pull out. The measured wear rate of DC-3 is much lower than that of DC-2 for which the dominant wear mechanism was fatigue. Although the mechanism associated with the wear of composite DC-1 was also fatigue, the composite's high fracture toughness and fatigue resistance retarded the wear particle formation reducing its wear rate. This observed fatigue wear behaviour of composites DC-1 and DC-2 is now considered using fracture mechanics.

As discussed in Sections 3.5 and 3.6, wear scar subsurface crack formation was observed in DC-1 and DC-2 specimens following wear testing. Due to the brittle nature of these composites [12], the tensile stress generated at the trailing edge of the cusp [34] can be considered responsible for the observed wear scar subsurface cracks. The progressive generation of the wear particles on these composite surfaces seem to indicate a mechanism of wear particle formation due to initiation of a crack and its subsequent propagation in a fatigue process. It is shown that the fatigue crack growth rate in polymers and dental composites can be related to the fracture mechanics parameters using the Paris law expressed as [10,35]

$$\frac{da}{dN} = A(\Delta K_I)^m \tag{1}$$

where ΔK_I is the stress intensity factor range ($\Delta K_I = K_{Imax} - K_{Imin}$) and, A and m are material constants. For the sliding contact conditions used in the present experiments, K_{Imin} is assumed to be 0.

According to Griffith's theory, the stress intensity factor, K_I, can be defined as

$$K_I = Y\sigma_a a^{1/2} \tag{2}$$

where Y is a geometrical factor and σ_a is the applied stress. From Eqs. (1) and (2), the number of cycles to form and remove a wear particle, N_f, may be expressed as [10]

$$N_f = \frac{a_f^{(-m/2)+1} - a_i^{(-m/2)+1}}{(-m/2+1)A\sigma_a^m Y^m} \tag{3}$$

where a_i and a_f are initial and final crack lengths under applied stress σ_a. The relation between fracture toughness of the composite K_{Ic}, and a_f can be expressed as

$$K_{Ic} = Y\sigma_a a_f^{1/2} \tag{4}$$

From Eq. (3), it can be seen that a larger value for a_i, due to debonding at the filler-matrix interface e.g., caused by hydrolytic degradation [10] or mechanical effects during grinding and/or polishing (Section 3.6) will reduce the number of cycles required to generate a wear particle. Additionally, a composite material that displays greater filler-matrix interface debonding possesses a lower short crack fracture toughness [10] and hence smaller a_f (Eq. (4)) and lower N_f (Eq. (3)) than one that resists such debonding e.g., composite DC-1. This explains why DC-2 (with a microstructure that revealed greater interface debonding) showed a much higher wear rate than DC-1 where only little interface debonding was observed.

A direct comparison of the wear rates for enamel-on-enamel and composite-on-composite situations are not possible because of the different lubricants used in the tests. However, the results in Fig.8 seem to indicate that, in general, composite-on-composite wear rates are lower than those for enamel-on-enamel. Based on the present results and analysis it is also possible to speculate the

wear behaviour of a composite in enamel-on-composite sliding contact situation.

It was noted that DC-1 and DC-2 tended to wear by subsurface crack propagation with a dominant fatigue wear mechanism. During enamel-composite contact in the oral environment, due to the much higher elastic modulus of enamel (and hence higher Hertzian contact stresses) compared to dental composites, it is possible that these dental composites, particularly DC-2, can wear at a higher rate than that observed in the present study. This is also supported by the observed dependency of the wear rate of DC-2 on the contact load (Fig. 8).

Using FIB/SEM, the present study has revealed subsurface damage of dental composites DC-1 and DC-2 from *in vitro* wear tests. A previous study has also reported subsurface damage (which was made visible by the silver staining process) in dental composite restorations worn *in vivo* [11].

The authors acknowledge that the number of cycles used during wear tests was relatively low and number of specimens used in the present study was relatively small compared to some of the previous studies. However, the number of wear cycles was selected to be similar to comparable studies involving human enamel which enabled comparison of present results with enamel wear. Additionally, the approach adopted in this study allowed an in-depth investigation of the associated wear mechanisms and interrelations among microstructure, mechanical properties and wear behaviour of dental composites which was the main focus of the study, rather than attempt to present general wear results. It was noted that some of the previous studies involving mechanistic structure and property relationships have also used a relatively smaller number of specimens, e.g., nanoindentation analysis in [36] and the nanometre scale scratching experiments in [37] have used only 6 specimens per study.

The present *in vitro* study investigated in-depth the wear behaviours in composite-on-composite sliding contact using analytical, electron microscopy and nanoindentation techniques. It has revealed the dominant wear mechanisms involved. The testing configuration and parameters were selected so that the experiments closely simulated the oral environment. There are nevertheless some constraints pertinent to the approach: use of a limited number of composite samples in wear tests restricted the quantitative analysis; *in vitro* environment compared to the general complexity of the oral environment consisting of fluids with changing composition and pH, and cyclic loads and thermal conditions.

5. Conclusions

From the present *in vitro* study of the wear behaviour of three different dental composite materials and subsequent electron microscopy and nanomechanical analyses, it was revealed that two different wear mechanisms were dominant for the composites under conditions tested (composite-on-composite sliding configuration; contact loads in the range 2–10 N; speed 66 cycles per minute; artificial saliva lubricant). These wear mechanisms were: fatigue wear mechanism for composites DC-1 and DC-2, and abrasion for DC-3. While fatigue wear caused extensive surface/subsurface microcrack formation/extension, abrasion was due to lateral crack extension and filler particle pull out.

Acknowledgements

The authors wish to thank Mr. Joshua Cheetham and SDI Ltd. (Melbourne, Vic) for providing the dental composite samples and financial support for a part of the experiments. They also gratefully acknowledge the assistance of Mr. W Joe during nanoindentation tests and useful discussions with Dr. C Kong during FIB/TEM investigations and access to the UNSW node of the Australian Microscopy & Microanalysis Research Facility (AMMRF).

References

[1] Z.R. Zhou, J. Zheng, Tribology of dental materials: a review, J. Phys. D: Appl. Phys. (2008) 41.
[2] P. Padipatvuthikul, F.D. Jarad, L. Mair, Determination of surface and subsurface fatigue damage in dental composites, Wear 268 (2010) 1483–1489.
[3] C.R. Perez, M.R. Gonzalez, N.A.S. Prado, M.S.F. deMiranda, M. de AndradeMaĉedo, B.M.P. Fernandes, Restoration of noncarious cervical lesions: when, why and how, Int. J. Dent. (2012), http://dx.doi.org/10.1155/2012/687058.
[4] J.L. Ferracane, Is the wear of dental composites still a clinical concern? Is there still a need for in vitro wear simulating devices?, Dent. Mater. 22 (2006) 689–692.
[5] Dijken van, Direct resin composite inlays/onlays: an 11 year follow-up, J. Dent. 28 (2000) 299–306.
[6] U. Pallesen, V. Qvist, Composite resin fillings and inlays, 11-year Eval. Clin. Oral. Invest 7 (2003) 71–79.
[7] J.T. Hamburger, Treatment of severe tooth wear – a minimally invasive approach (PhD Thesis), Radboud University, The Netherlands, 2014 ISBN 978-90-9028731-7 http://hdl.handle.net/2066/134182.
[8] J.T. Hamburger, N.J. Opdam, E.M. Bronkhorst, C.M. Kreulen, J.J. Roeters, M.C. Huysmans, Clinical performance of direct composite restorations for treatment of severe tooth wear, J. Adhes. Dent. 13 (6) (2011) 585–593.
[9] M. Braem, P. Lambrechts, V. van Doren, G. Vanherle, In vivo evaluation of four posterior composites: quantitative wear measurements and clinical behaviour, Dent. Mater. 2 (1986) 106–113.
[10] V.T. Truong, D.J. Cock, N. Padmanathan, Fatigue crack propagation in posterior dental composites and prediction of clinical wear, J. Appl. Biomater. 1 (1990) 21–30.
[11] J.E. McKinney, W. Wu, Relationship between subsurface damage and wear of dental restorative composites, J. Dent. Res 61 (9) (1982) 1083–1088.
[12] S.D. Heintze, G. Zellweger, G. Zappini, The relationship between physical parameters and wear of dental composites, Wear 263 (2007) 1138–1146.
[13] X. Hu, P.M. Marquis, A.C. Shortall, Two-body in vitro wear study of some current dental composites and amalgams, J. Prosthet. Dent. 82 (1999) 214–220.
[14] J.A. de Souza, L.C. Dolavale, S.A. de Souza Camargo, Wear mechanisms of dental composite restorative materials by two different in-vitro methods, Mater. Res. 16 (2) (2013) 333–340.
[15] J.R. Condon, J.L. Ferracane, Factors effecting dental composite wear *in vitro*, J. Biomed. Mater. Res (Appl. Biomater.) 38 (1997) 303–313.
[16] R. Lewis, R.S. Dwyer-Joyce, Wear of human teeth: a tribological perspective, Proc. Inst. Mech. Eng. Part J: J. Eng. Tribology 219 (2005) 1–18.

[17] S.D. Heintze, G. Zappini, V. Rousson, Wear of ten restorative materials in five wear simulators – results of a round robin test, Dent. Mater. 21 (2005) 304–317.
[18] C.P. Turssi, B. de Moraes Purquerio, M.C. Serra, Wear of dental resin composites: insights into underlying processes and assessment methods—a review, J. Biomed. Mater. Res Part B: Appl. Biomater. 65B (2003) 280–285.
[19] W.C. Oliver, G.M. Pharr, An improved technique for determining hardness and elastic modulus using load and displacement sensing indentation experiments, J. Mater. Res 1992 (7) (1992) 1564–1583.
[20] N.E. Waters, Some mechanical and physical properties of teeth, in: J. Vincent, J. Curry (Eds.), The Mechanical Properties of Biological Materials, Cambridge University Press, Cambridge, 1980, pp. 99–134.
[21] J. Zheng, Z.R. Zhou, Study of *in vitro* wear of human tooth enamel, Tribology Lett. 26 (2007) 181–189.
[22] J.A. Arsecularatne, M. Hoffman, An *in vitro* study of the microstructure, composition and nanoindentation mechanical properties of remineralising human dental enamel, J. Phys. D: Appl. Phys. (2014), http://dx.doi.org/10.1088/0022-3727/47/31/315403.
[23] A. Ramalho, A reliability model for friction and wear experimental data, Wear 269 (2010) 213–223.
[24] J.A. Arsecularatne, J.P. Dingeldein, M. Hoffman, An *in vitro* study of the wear mechanism of a leucite glass dental ceramic, Biosurf. Biotribol. 1 (2015) 50–61.
[25] Y.Q. Wu, J.A. Arsecularatne, M. Hoffman, Effect of acidity upon attrition-corrosion of human dental enamel, J. Mech. Behav. Biomed. Mater. 44 (2015) 23–34.
[26] M. Eisenburger, M. Addy, Erosion and attrition of human enamel *in vitro* Part II: influence of time and loading, J. Dent. 30 (2002) 349–352.
[27] W.S. Oh, R. DeLong, K. Anusavice, Factors affecting enamel and ceramic wear: a literature review, J. Prosthet. Dent. 87 (2002) 451–459.
[28] S. Hahnel, S. Schultz, C. Trempler, B. Ach, G. Handel, M. Rosentritt, Two-body wear of dental restorative materials, J. Mech. Behav. Biomed. Mater. 4 (2011) 237–244.
[29] J.A. Arsecularatne, M. Hoffman, On the wear mechanism of human dental enamel, J. Mech. Behav. Biomed. Mater. 3 (2010) 347–356.
[30] F.F. Lange, K.C. Radford, Fracture energy of an epoxy composite system, J. Mater. Sci. 6 (1971) 1197–1203.
[31] A.C. Moloney, H.H. Kausch, H.R. Stieger, The fracture of particulate filled epoxide resins, J. Mater. Sci. 19 (1984) 1125–1130.
[32] J.A. Arsecularatne, M. Hoffman, Ceramic-like wear behaviour of human dental enamel, J. Mech. Behav. Biomed. Mater. 8 (2012) 47–57.
[33] U. Lohbauer, R. Belli, J.L. Ferracane, Factors involved in mechanical fatigue degradation of dental resin composites, J. Dent. Res. 92 (2013) 584–591.
[34] G.M. Hamilton, Explicit equations for the stresses beneath a sliding spherical contact, Proc. Inst. Mech. Eng. Part C 197 (1983) 53–58.
[35] A.J. Kinloch, R.J. Young, Fracture Behaviour of Polymers, Applied Science Publisher, London and New York, 1983.
[36] J.L. Cuy, A.B. Mann, K.J. Livi, M.F. Teaford, T.P. Weihs, Nanoindentation mapping of the mechanical properties of human molar tooth enamel, Arch. Oral. Biol. 47 (2002) 281–291.
[37] G.M. Guidoni, M.V. Swain, I. Jager, Wear behaviour of dental enamel at the nanoscale with sharp and blunt indenter tip, Wear 266 (2008) 60–68.